Research Square

Preprints are preliminary reports that have not undergone peer review.
They should not be considered conclusive, used to inform clinical practice,
or referenced by the media as validated information.

Separating hot-dry hazard burden from amplification in Zambia from 1996 to 2025

Siatwiinda Mabele Siatwiinda

ssiatwiinda@mu.edu.zm

Mulungushi University

Research Article

Keywords: compound events, hot-dry extremes, CHIRPS, ERA5-Land, ENSO, Zambia

Posted Date: November 10th, 2026

DOI: https://doi.org/10.21203/rs.3.rs-11194034/v1

License: This work is licensed under a Creative Commons Attribution 4.0 International License.
Read Full License

Additional Declarations: No competing interests reported.

Separating hot-dry hazard burden from amplification in Zambia from 1996 to 2025

Siatwiinda Mabele Siatwiinda[1*]
* Corresponding author email address: ssiatwiinda@mu.edu.zm or siatwiindamabele@yahoo.com
[1]Mulungushi University, P.O Box 80415, Kabwe, Zambia.

Abstract

Compound hot-dry hazards may intensify because heat or dryness becomes more prevalent, or their dependence strengthens, or because hazardous days cluster into persistent events. These pathways are obscured when change is assessed from event counts alone. Here, a burden-amplification framework separates realized event burden from excess heat-dryness co-occurrence. The framework was applied to 30 November-March growing seasons ending in 1996-2025 across Zambia using CHIRPS rainfall, ERA5-Land maximum temperature and fixed 1986-2014 local thresholds. Event burden was characterized by frequency, affected days, duration and severity, while amplification measured observed joint occurrence relative to that expected from separate hot- and dry-day probabilities. Event frequency showed no robust linear increase (0.173 events per decade; 95% confidence interval, −0.133 to 0.489), although 2023/24 strongly influenced recent burden. Decomposition identified increasing hot-day prevalence as the dominant positive component (+21.24% per decade; 95% block-bootstrap confidence interval, 1.15 to 45.19), while dry-day prevalence made a smaller, uncertain contribution (+3.15%; −1.35 to 7.81). Amplification declined by 6.08% per decade (−8.76 to −3.05), offsetting approximately 39% of the net log-scale change. Consequently, the estimated increase in joint occurrence remained uncertain (+17.46%; −6.56 to 47.32). The exceptionally high burden but low amplification of 2023/24 demonstrates that more hazard need not imply stronger dependence. Separating marginal prevalence, realized burden and amplification can provide a more informative basis for monitoring compound hazards within and beyond Zambia.

Keywords: compound events; hot-dry extremes; CHIRPS; ERA5-Land; ENSO; Zambia

[1] Mulungushi University, P.O Box 80415, Kabwe, Zambia.

1 Introduction

Climate hazards rarely occur as isolated stresses (Leonard et al. 2014; AghaKouchak et al. 2020). High temperature may coincide with rainfall deficits, prolonged dryness may be followed by intense rainfall, and several moderate conditions may combine to produce consequences greater than those associated with any component alone (Lesk et al. 2022; Ebi 2025). These compound events are increasingly important in climate-risk research because their impacts depend on the interaction, sequencing and duration of the contributing hazards (Ebi 2025; Zscheischler et al. 2018; Zscheischler et al. 2020). In rain-fed agricultural systems, for example, rainfall deficits reduce soil-water availability while high temperatures raise atmospheric water demand, accelerate crop water loss and can shorten critical stages of crop development (Lesk et al. 2022; Zhang et al. 2023). Intense rainfall after an extended dry spell may then generate runoff and erosion without fully restoring plant-available water (Trnka et al. 2016; Cao et al. 2025). Understanding such combinations is therefore important for seasonal monitoring, early warning and agricultural risk management.

The growing literature on compound extremes has improved the identification of multivariate and temporally connected hazards, but an important interpretive challenge remains (Zscheischler et al. 2018; Zscheischler et al. 2020; Hao et al. 2018b; AghaKouchak et al. 2020; White et al. 2025). Event frequency, affected days, event duration, severity, joint probability and statistical dependence describe different properties of a hazard record (Al-Wardy et al. 2026). They may move in the same direction, but they need not do so. A season can contain many hot-dry days simply because hot conditions have become more common, even if heat is no more likely than before to occur specifically during dry conditions. Conversely, a strong statistical association between heat and dryness can occur in a season with relatively few events. Treating these measures as interchangeable can obscure the physical structure of change and complicate communication with decision-makers.

This distinction matters because the phrase “increasing compound hazard” can describe several different developments (Al-Wardy et al. 2026). More events may result from an increase in the prevalence of heat, an increase in the prevalence of dryness, a strengthening of their dependence, or some combination of these processes. Apparent trends can also be shaped by a small number of exceptional seasons, particularly when observational records are only a few decades long. An analysis based only on event counts or joint probabilities cannot determine which component dominates (Vogel et al. 2024). It may correctly show that exposure increased while inadvertently suggesting that the contributing hazards became more tightly connected. For monitoring purposes, the amount of hazard experienced and the dependence between its components should therefore be reported separately.

This study addresses the problem through a burden-amplification framework. Event burden describes the amount of hazard realised through event frequency, affected days, duration and severity, whereas amplification measures how often heat and dryness co-occur relative to the frequency expected from their separate occurrence. The decomposition follows established approaches that distinguish changes in marginal probabilities from changes in dependence within compound events (Bevacqua et al. 2019; François and Vrac 2023) (Equation 1):

$$A = \frac{P(H \cap D)}{P(H) \cdot P(D)} \qquad \text{Eqn 1}$$

where H denotes a hot day and D denotes a dry day.

A value above one indicates positive dependence, but it does not by itself imply a large absolute burden: if hot or dry days are rare, their joint occurrence can remain uncommon even when amplification is high. Likewise, a high burden does not necessarily require rising amplification when one of the component hazards becomes sufficiently prevalent.

The probability identity equation 2 provides an exact way to separate these components. On a logarithmic scale, change in joint occurrence can be expressed as the sum of changes in hot-day prevalence, dry-day prevalence and amplification.

$$P(H \cap D) = P(H) \times P(D) \times A \qquad \text{Eqn 2}$$

This approach follows methods that attribute compound-hazard probability change to marginal and dependence contributions, most directly demonstrated for compound coastal flooding from precipitation and storm surge (Bevacqua et al. 2019) and subsequently formalized within a copula-based framework for other compound climate hazards (François and Vrac 2023). This decomposition is descriptive rather than causal. It identifies which statistical component contributed to the observed joint trend but does not establish the atmospheric, land-surface or socioeconomic mechanism responsible for that component. Event burden is also related to, but not mathematically identical to, daily joint probability because qualifying events depend on the temporal clustering of hot and dry days into sustained spells (Figure 1). The framework consequently links two questions that are often merged, how much compound hazard occurred, and how unusually strongly did its components coincide?

Separating these questions is especially useful in regions with strong year-to-year climate variability. Southern African droughts are often accompanied by high temperatures, but their timing, magnitude and spatial expression differ among seasons (Lyon 2009). The El Niño-Southern Oscillation influences regional rainfall and circulation, although its effects are not uniform and can depend on the configuration of Pacific and Indian Ocean conditions (Hao et al. 2018a; Hoell et al. 2015). The 2023/24 El Niño coincided with widespread rainfall failure and severe disruption across southern Africa (Moses et al. 2025). Preliminary attribution evidence identified El Niño as an important contributor to the 2023/24 drought, alongside long-term warming and pre-existing vulnerability (Sparrow et al. 2026). Exceptional seasons of this kind can dominate short trend records and provide a useful test of whether high burden necessarily corresponds to stronger heat-dryness dependence.

Zambia provides a policy-relevant setting for this test. Crop production, livestock systems, hydropower generation and many rural livelihoods depend heavily on the November-March rainy season (Mulungu et al. 2026; Hamududu and Ngoma 2019). Zambia also spans contrasting agro-ecological zones, from the relatively dry south and west to wetter northern areas, so a national average may conceal important regional differences (Siatwiinda et al. 2021). A season with widespread hot-dry spells can affect planting, crop establishment, flowering and water availability, but the climate metrics examined here represent hazards rather than measured losses. Their practical value lies in describing the timing and spatial distribution of potentially damaging conditions, not in assuming a direct or uniform effect on yields, livelihoods or infrastructure.

Previous work in Zambia and the wider region has commonly assessed drought through rainfall anomalies, the Standardized Precipitation Index or the Standardized

Precipitation Evapotranspiration Index, while temperature and rainfall extremes are frequently analysed in separate assessments (Chisanga et al. 2023; Libanda et al. 2020; Hachigonta et al. 2008; Tirivarombo et al. 2018; Chisanga et al. 2025). These approaches remain valuable for characterizing meteorological drought and long-term climate tendencies. However, they do not directly show whether hot days occurred within sustained dry spells, whether prolonged dryness was followed by extreme rainfall, or whether a change in joint hot-dry occurrence was driven mainly by the individual hazards or by their dependence. A spell-based analysis combined with probability decomposition can therefore provide information that is complementary to, rather than a repetition of, standardized drought analysis.

Using 30 complete growing seasons ending between 1996 and 2025, this study examines whether the burden of hot-dry events changed steadily or episodically and whether heat-dryness amplification strengthened or weakened. It also assesses how changes in hot-day prevalence, dry-day prevalence and amplification contributed to joint hot-dry occurrence. The study further investigates whether seasons with a high event burden necessarily experienced high amplification and tests whether the findings were sensitive to alternative event definitions, major El Niño seasons and changes in data coverage.

Zambia is treated as an empirical test case for a broader analytical proposition: changes in compound-hazard burden should not automatically be interpreted as changes in dependence. The study is observational and does not attribute the detected patterns to individual climate drivers. Its contribution is a transparent and transferable framework for distinguishing the scale of compound hazard from the statistical relationship between its components.

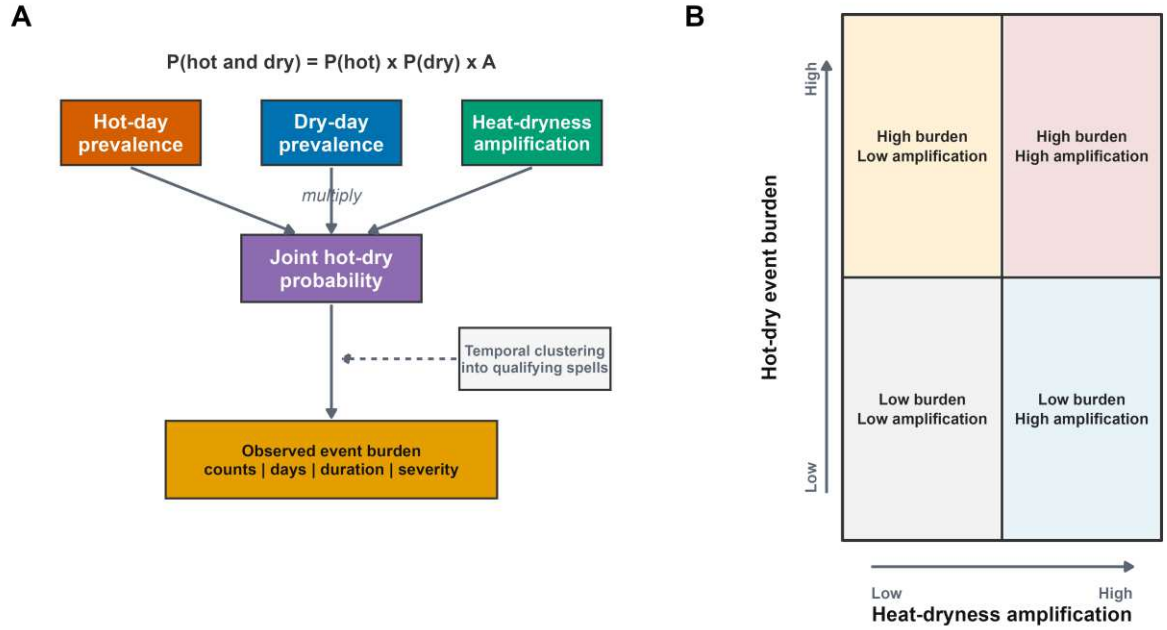


Figure 1: Burden-amplification framework for compound hot-dry hazards. A) Decomposes joint occurrence into hot-day prevalence, dry-day prevalence and heat-dryness amplification, with event burden also shaped by temporal clustering. B) Four descriptive burden-amplification states. These states are not universal hazard thresholds.

2 Methods

2.1 Study area

Zambia is a landlocked southern African country (between latitudes 8 °S and 18 °S and longitudes 22 °E and 34 °E) of approximately 752600 km^2. Its unimodal rainy season generally extends from November to March or April, with a strong south-to-north rainfall gradient. Zambia is divided into Agro-Ecological Regions I, IIa, IIb and III using the official national agro-ecological classification. The analysis used the national boundary and four agricultural zones: AEZ I, IIa, IIb and III. AEZ I is comparatively dry and drought-prone; AEZ IIa includes much of the central and eastern maize-producing belt; AEZ IIb covers western areas with sandy soils and distinct production constraints; and AEZ III is the wetter northern zone. National and zonal estimates were weighted by grid-cell area calculated on the ERA5-Land analysis grid.

2.2 Observational data and season construction

Daily precipitation was obtained from the Climate Hazards Infrared Precipitation with Stations dataset (CHIRPS) (Funk et al. 2015). Daily maximum temperature was derived from hourly ERA5-Land two-metre temperature (Muñoz-Sabater et al. 2021) by converting Kelvin to degrees Celsius and taking the daily maximum. A single 0.1-degree geographic analysis grid was defined from the January 1985 ERA5-Land layer, cropped and masked to Zambia. Every precipitation and temperature layer was aligned to this template before stacking. The CHIRPS precipitation was aggregated using area averaging, while the continuous ERA5-Land temperature field used bilinear interpolation. This fixed-grid procedure addressed fractional differences in extent or origin between the legacy 1985-2014 and updated 2015-2025 ERA5-Land processing archives. Each growing season comprised November and December of the preceding calendar year and January-March of the labelled ending year, for example, season 1996 comprised November-December 1995 and January-March 1996. The trend analysis covered seasons ending in 1996-2025. Cells were retained for annual event calculation when at least 90% of daily precipitation and temperature observations were jointly valid. Values below this completeness threshold were treated as missing rather than imputed. Fixed thresholds were estimated from all complete November-March seasons ending in 1986-2014.

Using a fixed baseline prevents the threshold from adapting to recent warming and ensures that trends reflect changing exceedance frequency relative to a common historical reference. At each cell, a hot day exceeded the local 90th percentile of daily maximum temperature. A dry day had precipitation below 1 mm. Extreme rainfall exceeded the local 95th percentile calculated from baseline wet days with precipitation of at least 1 mm. Both percentile thresholds used the Type 8 sample-quantile estimator implemented in R.

2.3 Compound-event metrics

Compound-event metrics were adapted from previous spell-based assessments of hot and dry hazards (Szalińska et al. 2021; Majid and Fethi 2024; He et al. 2022).

A hot-dry event was defined as a dry spell lasting at least five consecutive days and containing at least three locally hot days. Event frequency was the number of qualifying spells. Hot-dry days were the hot days occurring within those spells. Maximum duration was the length of the longest qualifying dry spell. Severity was the cumulative temperature exceedance above the local heat threshold during qualifying events, expressed in degree-days ($°C^{-day}$).

Dry-to-wet transitions counted dry spells lasting at least seven days that were followed within seven days by rainfall above the local wet-day 95th percentile. A multihazard-season indicator equalled one when a season contained both a hot-dry event and a dry-to-wet transition. Hot-dry amplification was calculated as P(hot and dry)/[P(hot)P(dry)] from all valid growing-season days. A value of one indicates that the two conditions occurred together as often as expected from their separate frequencies, a value above one indicates excess co-occurrence. Maximum duration measures the entire qualifying dry spell rather than only its hot-day subset. Amplification was undefined where either marginal probability was zero and was stored as missing rather than assigned a numerical value. National and AEZ means omitted undefined cells and renormalized area weights over cells with defined amplification in each season. This mathematical undefinedness was tracked separately from climate-data availability.

2.4 Trend and nonlinear-change analysis

Area-weighted national and AEZ annual series were analysed over 1996-2025. Linear monotonic change was estimated with the Sen slope. Uncertainty was quantified from 2000 moving-block bootstrap replicates that resampled five-season blocks of residuals around the fitted Sen trend, thereby preserving short-run temporal dependence (Wilks 1997). Five-season blocks were used to preserve short-term temporal dependence while retaining enough resampled blocks within the 30-season record. Modified Mann-Kendall tests adjusted the test variance for significant autocorrelation in Sen-detrended ranks (Hamed and Ramachandra Rao 1998). Generalized least-squares models fitted by restricted maximum likelihood with first-order autoregressive errors provided a parametric slope and complementary significance test (Pinheiro and Bates 2000). Generalized additive models (GAMs) fitted by restricted maximum likelihood used a penalized smooth with basis dimension selected from the available number of seasons to describe nonlinear trajectories (Wood 2025). The GAMs were treated as descriptive smoothers rather than process models, and endpoint differences are fitted contrasts across a short, shock-rich record rather than observed causal effects. National tests were prespecified. The four AEZs formed a separate exploratory family within each metric, for which Benjamini-Hochberg adjustment controlled the false-discovery rate (Benjamini and Hochberg 1995). Evidence was classified from the agreement among slope direction, bootstrap intervals, modified Mann-Kendall results, GLS-AR(1) estimates and GAM shape. Statistical inference was not reduced to a single p-value. A trend was described as robust when direction agreed across methods, the bootstrap interval excluded zero and the primary test met its prespecified error-control criterion. Nonlinear change was classified when the GAM effective degrees of freedom exceeded 1.10 and the national GAM p-value, or the Benjamini-Hochberg-adjusted q-value for the Agro-ecological zones, was below 0.05.

2.5 Spatial trends

Cell-level Sen slopes and modified Mann-Kendall p-values were calculated for each metric over 1996-2025. Benjamini-Hochberg correction was applied across valid grid cells. Area-weighted national slopes and the proportions of Zambia with significant positive or negative trends were then calculated. These maps distinguish areas with detectable cell-wise change from areas where the 30-season record provides insufficient evidence. Non-significance was not interpreted as evidence of no change.

2.6 ENSO and archive-boundary sensitivity

Growing seasons ending in 1998, 2016 and 2024 represented the 1997/98, 2015/16 and 2023/24 major El Niño events. GLS-AR(1) models were refitted after excluding each season separately and all three together. Additional models included a linear trend, a post-2015 indicator and individual El Niño indicators. The 2015 term was treated as a diagnostic rather than automatic evidence of a processing artefact. Candidate step years from 2002 to 2019 were also scanned exploratorily using Akaike's information criterion (Akaike 1974), with these results kept separate from confirmatory inference.

2.7 Input-continuity and common-domain sensitivity

Because the processed ERA5-Land footprint became slightly smaller after 2015, input-level GLS-AR(1) models tested a post-2015 step after accounting for temporal trend and calendar month in national mean temperature, upper-tail temperature and CHIRPS precipitation. A final common-domain analysis intersected valid ERA5-Land source cells across all 150 monthly inputs supporting the 1996-2025 November-March seasons. National and AEZ annual series and trends were re-estimated on this fixed source domain. Fractional polygon coverage and grid-cell area were used for the common-domain coverage audit. Metric-specific undefined values were not used to define climate-data coverage. Grid-cell OLS slopes calculated independently with Climate Data Operators provided an additional computational comparison (Schulzweida et al. 2019).

2.8 Event-definition and influential-season sensitivity

Event-definition uncertainty was evaluated using four alternatives to the primary five-dry-day, three-hot-day and local P90 definition.

The alternatives comprised a four-day spell containing at least two hot days, a six-day spell containing at least three hot days, and five-day/three-hot-day events defined using local P85 or P95 temperature thresholds. The 1 mm dry-day threshold was held constant so that the sensitivity isolated event-duration, hot-day-count and heat-threshold choices. Fixed P85, P90 and P95 thresholds were all estimated with Type 8 quantiles from the 1986-2014 baseline. For each definition, national and AEZ annual series were recalculated from the daily data, followed by Sen, GLS-AR(1) and descriptive GAM analyses. Since amplification is defined from daily marginal and joint probabilities rather than qualifying spell counts, changing only the spell-length rule does not alter that metric. GAMs were also refitted after excluding the 2023/24 season. Finally, 95% confidence intervals were calculated for the 1997/98, 2015/16 and 2023/24 indicator coefficients in models containing linear time, a post-2015 term and AR(1) errors.

2.9 Burden-amplification decomposition

For each season and region, area-weighted P(hot), P(dry) and P(hot and dry) were calculated from the annual cell-level probability rasters. Regional amplification was then defined as P(hot and dry)/[P(hot)P(dry)]. This ratio of regionally aggregated probabilities differs from the primary area-weighted mean of cell-level ratios, but it is required for an exact regional decomposition. All three probabilities were calculated over a fixed valid area. On the log scale, the identity becomes:

$$\log P(H \cap D) = \log P(H) + \log P(D) + \log A \qquad \text{Eqn 3}$$

Ordinary least-squares (OLS) slopes over 1996-2025 were estimated for the three components and their sum, expressed per decade. OLS was used because the component slopes add exactly on the log scale. Percentage changes were calculated as:

$$\%\Delta = 100[\exp(\beta) - 1] \quad \text{Eqn 4}$$

where β is the estimated decadal slope. Uncertainty was estimated from 2000 moving-block bootstrap replicates with five-season blocks. Residual vectors for the three components were resampled jointly, preserving their covariance and short-run temporal structure. Separate GLS-AR(1) slopes were fitted as sensitivity checks but were not required to add exactly because each model estimated its own correlation structure. Component contributions were also expressed as percentages of the net log change; negative contributions represent offsets, and values above 100% can occur when opposing components reduce the net change. For descriptive interpretation, each region-season was additionally located in a burden-amplification plane using hot-dry days as the burden measure and regionally aggregated amplification as the dependence measure. Region-specific 1996-2025 medians divided the plane into high- and low-burden and high- and low-amplification states. These median-based states were used only as diagnostic summaries and were not treated as physical, agronomic or statistical hazard thresholds. The primary trend analysis used an area-weighted mean of cell-level amplification ratios. The exact decomposition instead required regionally aggregated amplification, calculated as the ratio of aggregated joint probability to the product of aggregated marginal probabilities. These measures answer related but different questions and were not treated as interchangeable.

3 Results

3.1 Hot-dry burden varied episodically rather than increasing steadily

A typical growing season across Zambia contained 1.13 hot-dry events and 7.86 hot-dry days (Table 1). Neither measure showed a consistent linear increase between 1996 and 2025. Event frequency increased by an estimated 0.173 events per decade, but the confidence interval crossed zero (95% CI, −0.133 to 0.489; modified Mann-Kendall p = 0.269). The GLS estimate was similarly uncertain (0.244 events per decade; p = 0.123). Hot-dry days increased by 0.628 days per decade according to the Sen estimate (95% CI, −2.128 to 3.081), whereas the GLS estimate was 1.285 days per decade (p = 0.265).

Nonlinear models nevertheless detected temporal structure in event frequency (edf = 2.68, p = 0.007) and hot-dry days (edf = 2.79, p = 0.010). Fitted values for 2025 exceeded those for 1996 by 0.801 events and 2.54 hot-dry days. These changes were concentrated in particular seasons rather than distributed as steady increases across the record (Figure 2).

Event duration and severity showed similarly weak linear trends. Maximum event duration averaged 7.15 days, with a Sen slope of 0.180 days per decade (95% CI, −1.567 to 1.892) and a GLS slope of −0.005 days per decade (p = 0.996). Seasonal severity averaged 18.16 degree-days above the local heat threshold. Its estimated trend was positive but uncertain under both Sen (3.10 degree-days per decade; 95% CI, −4.13 to 10.50) and GLS models (1.89 degree-days per decade; p = 0.613).

Dry-to-wet transitions were uncommon and showed no sustained national trend. Zambia averaged 0.176 transitions per season, with a Sen slope of −0.021 transitions per decade (95% CI, −0.059 to 0.014) and a GLS slope of −0.019 per decade (p =

0.363). The area-weighted proportion of seasons containing both a hot-dry event and a dry-to-wet transition averaged 0.131. Both methods estimated a decline of approximately 0.015 per decade, but neither estimate was statistically resolved. Overall, compound-hazard burden varied markedly among seasons without showing uniform long-term escalation.

Table 1: National trends in observed compound-hazard metrics during 1996-2025. Slopes are expressed per decade. Confidence intervals were estimated using a moving-block bootstrap.

Metric	Mean	Sen slope decade^{-1}	95% bootstrap CI	GLS-AR1 slope decade^{-1}	GLS p	GAM edf	GAM p
Events	1.126	0.173	-0.133 to 0.489	0.244	0.123	2.68	0.007
Days	7.86	0.628	-2.128 to 3.081	1.285	0.265	2.79	0.01
Maximum duration	7.151	0.18	-1.567 to 1.892	-0.005	0.996	3.37	0.025
Severity	18.156	3.101	-4.130 to 10.497	1.889	0.613	3.32	0.004
Mean cell-level amplification	1.796	-0.092	-0.148 to -0.029	-0.086	0.01	1	0.02
Dry-to-wet transitions	0.176	-0.021	-0.059 to 0.014	-0.019	0.363	1.74	0.337
Multihazard season	0.131	-0.015	-0.049 to 0.019	-0.015	0.487	2.04	0.241

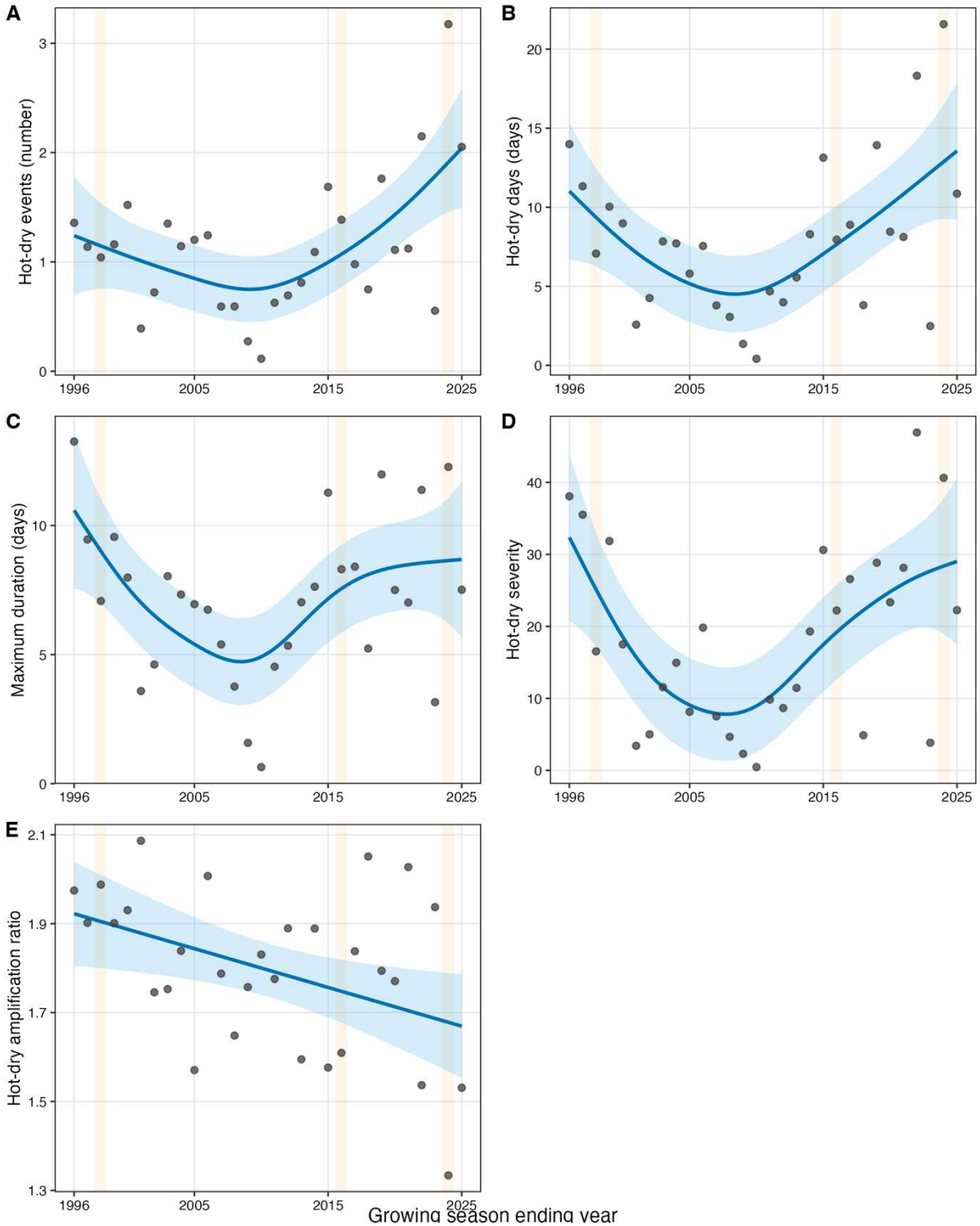


Figure 2: National compound hot-dry hazard trajectories, 1996-2025. a) Event frequency. b) Hot-dry days. c) Maximum duration. d) Severity. e) Mean cell-level amplification. Curves show GAM fits with 95% confidence intervals; major El Niño seasons are highlighted.

3.2 Heat-dryness amplification declined unevenly across Zambia

The clearest national change occurred in heat-dryness amplification rather than event burden (Figure 3). The mean amplification ratio was 1.796, indicating that hot and dry conditions occurred together approximately 1.8 times as often as expected from their separate frequencies. Amplification declined by 0.092 per decade (95% CI, −0.148 to −0.029; modified Mann-Kendall p = 0.038), with a similar GLS estimate of −0.086 per

decade (p = 0.010). The generalized additive model indicated an approximately linear decline (p = 0.020), corresponding to a fitted reduction of 0.253 between 1996 and 2025.

Table 2: Regional trends in mean cell-level heat–dryness amplification. National inference was prespecified; AEZ p-values were adjusted together using the Benjamini–Hochberg procedure.

Region	Sen slope decade-1	95% bootstrap CI	Modified MK p	AEZ-family q	GLS-AR1 slope decade-1	GLS p
Zambia	-0.092	-0.148 to -0.029	0.038	-	-0.086	0.01
AEZ I	-0.106	-0.146 to -0.061	<0.001	<0.001	-0.112	<0.001
AEZ IIa	-0.141	-0.226 to -0.055	0.025	0.049	-0.127	0.007
AEZ IIb	-0.131	-0.185 to -0.052	0.080	0.107	-0.132	0.02
AEZ III	-0.045	-0.116 to 0.027	0.284	0.284	-0.048	0.297

The decline varied across agro-ecological zones (Table 2). Amplification declined by 0.106 per decade in AEZ I (95% CI, −0.146 to −0.061; q < 0.001) and by 0.141 per decade in AEZ IIa (95% CI, −0.226 to −0.055; q = 0.049). The corresponding GLS estimates were −0.112 and −0.127 per decade. AEZ IIb showed a decline of comparable magnitude (−0.131 per decade; 95% CI, −0.185 to −0.052), although support differed between the adjusted rank-based test (q = 0.107) and the GLS model (p = 0.020). The smaller decline in AEZ III was not statistically resolved (−0.045 per decade; 95% CI, −0.116 to 0.027).

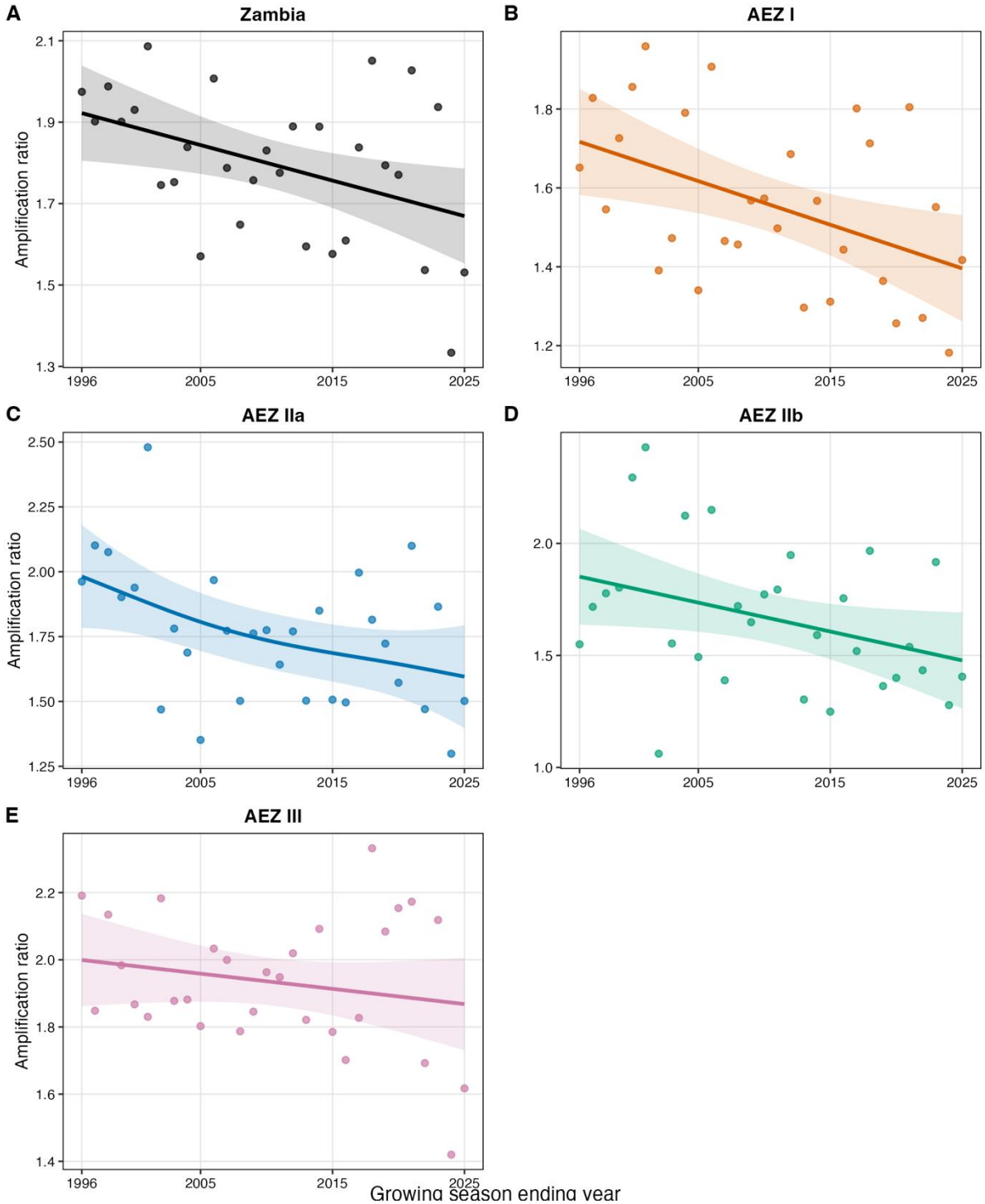


Figure 3: Heat–dryness amplification across Zambia and its agro-ecological zones. a, Zambia. b, AEZ I. c, AEZ IIa. d, AEZ IIb. e, AEZ III. Lines show fitted trends with 95% confidence intervals.

Grid-cell trends revealed distinct spatial structures among the four metrics (Figure 4). Event-frequency increases were sparse and concentrated in southern and southeastern Zambia (Figure 4a). Hot-dry days increased across much of the south and south-central regions but declined across parts of northern and northeastern Zambia (Figure 4b). Severity showed a similar spatial contrast, with positive slopes dominating the south and southeast and negative slopes occurring in parts of western, northern and northeastern Zambia (Figure 4c).

Amplification showed the most coherent spatial signal (Figure 4d). Negative slopes extended across much of western, central and southern Zambia, spanning large parts of AEZ I, AEZ IIa and AEZ IIb. Positive slopes were concentrated mainly in northern and northeastern Zambia, particularly in AEZ III. Significant declines clustered across west-central, central and southern areas, whereas significant increases were sparse and largely confined to the north. This pattern was consistent with the strong regional declines in AEZ I and AEZ IIa and the weaker trend in AEZ III.

The area-weighted amplification slope was −0.0917 per decade. Significant declines covered 10.57% of Zambia, compared with 0.23% for significant increases. By contrast, less than 0.1% of the country showed significant trends in event frequency, hot-dry days or severity. Declining amplification therefore provided the clearest spatial signal, whereas changes in event burden were heterogeneous and rarely resolved at the grid-cell scale.

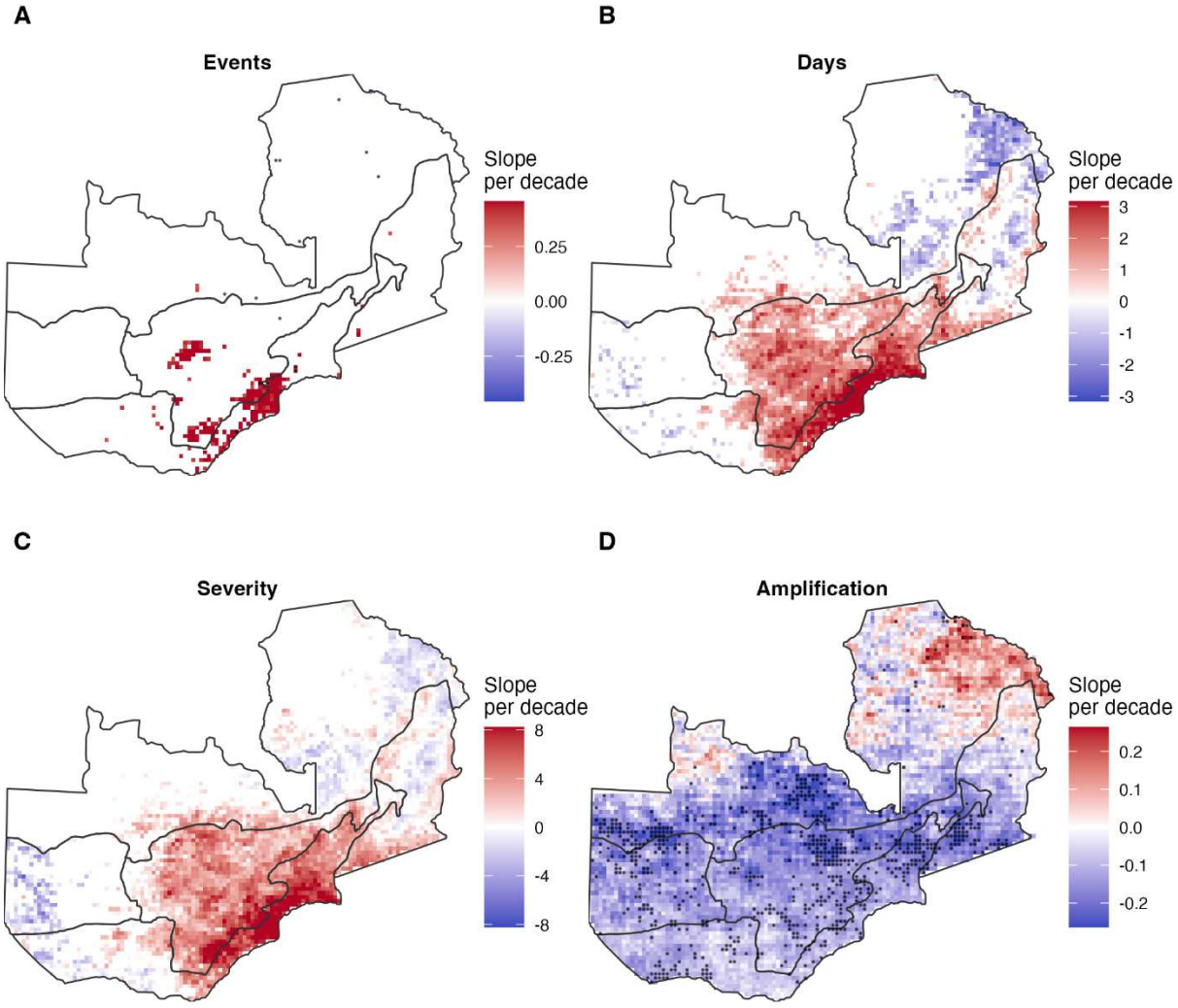


Figure 4: Spatial trends in compound hot-dry hazards, 1996–2025. Cell-wise Sen slopes for a) event frequency, b) hot-dry days, c) severity and d) mean cell-level amplification. Stippling identifies cells passing the field-wide false-discovery-rate threshold; lines delineate Agro-ecological zones.

3.3 Increasing hot-day prevalence dominated the change in joint occurrence

Decomposition showed that increasing hot-day prevalence was the principal positive component of change in joint hot-dry probability (Figure 5). National hot-day prevalence increased by 21.24% per decade (95% block-bootstrap CI, 1.15-45.19%;

p = 0.038)(Table 3). Dry-day prevalence increased by 3.15% per decade, but the estimate remained uncertain (95% CI, −1.35 to 7.81%; p = 0.163). Amplification declined by 6.08% per decade (95% CI, −8.76 to −3.05%; p < 0.001). These opposing components produced an estimated 17.46% increase per decade in joint hot-dry probability, but the confidence interval crossed zero (95% CI, −6.56 to 47.32%; p = 0.173). On the log scale, hot-day prevalence contributed 119.7% of the net positive estimate and dry-day prevalence contributed 19.3%, while declining amplification offset 39.0%. GLS-AR(1) models produced similar component slopes, although support for increasing hot-day prevalence was weaker (p = 0.093) and joint occurrence remained uncertain (p = 0.239).

Table 3: Decomposition of joint hot-dry probability change, expressed as percentage change per decade with 95% joint block-bootstrap intervals. Percentages are transformations of exact log-scale components. Intervals crossing zero indicate that the component trend was not statistically resolved

Region	Hot-day prevalence	Dry-day prevalence	Amplification	Joint occurrence
Zambia	21.24 (1.15, 45.19)	3.15 (-1.35, 7.81)	-6.08 (-8.76, -3.05)	17.46 (-6.56, 47.32)
AEZ I	26.00 (-0.95, 61.01)	4.16 (-0.84, 9.70)	-6.75 (-9.01, -4.38)	22.39 (-7.98, 64.52)
AEZ IIa	24.93 (1.28, 55.44)	4.78 (0.56, 9.47)	-7.94 (-11.82, -4.29)	20.51 (-6.18, 55.30)
AEZ IIb	33.65 (7.59, 61.64)	2.70 (-3.94, 9.80)	-7.46 (-10.20, -4.24)	27.02 (-2.74, 63.35)
AEZ III	17.36 (-0.31, 38.07)	1.55 (-2.42, 5.97)	-3.87 (-7.40, -0.35)	14.57 (-5.42, 39.97)

Hot-day prevalence was the largest positive component in every agro-ecological zone, increasing by 17.36% per decade in AEZ III to 33.65% in AEZ IIb (Figure 5 and Table 3). Amplification declined in all four zones, with the largest reduction in AEZ IIa (−7.94% per decade; 95% CI, −11.82 to −4.29%). AEZ IIa also showed increases in hot-day prevalence of 24.93% (95% CI, 1.28-55.44%) and dry-day prevalence of 4.78% per decade (95% CI, 0.56-9.47%). Nevertheless, confidence intervals for joint occurrence crossed zero nationally and in every AEZ. The decomposition therefore identified the components of observed change without establishing a uniform increase in joint occurrence or attributing the trends to specific causal processes.

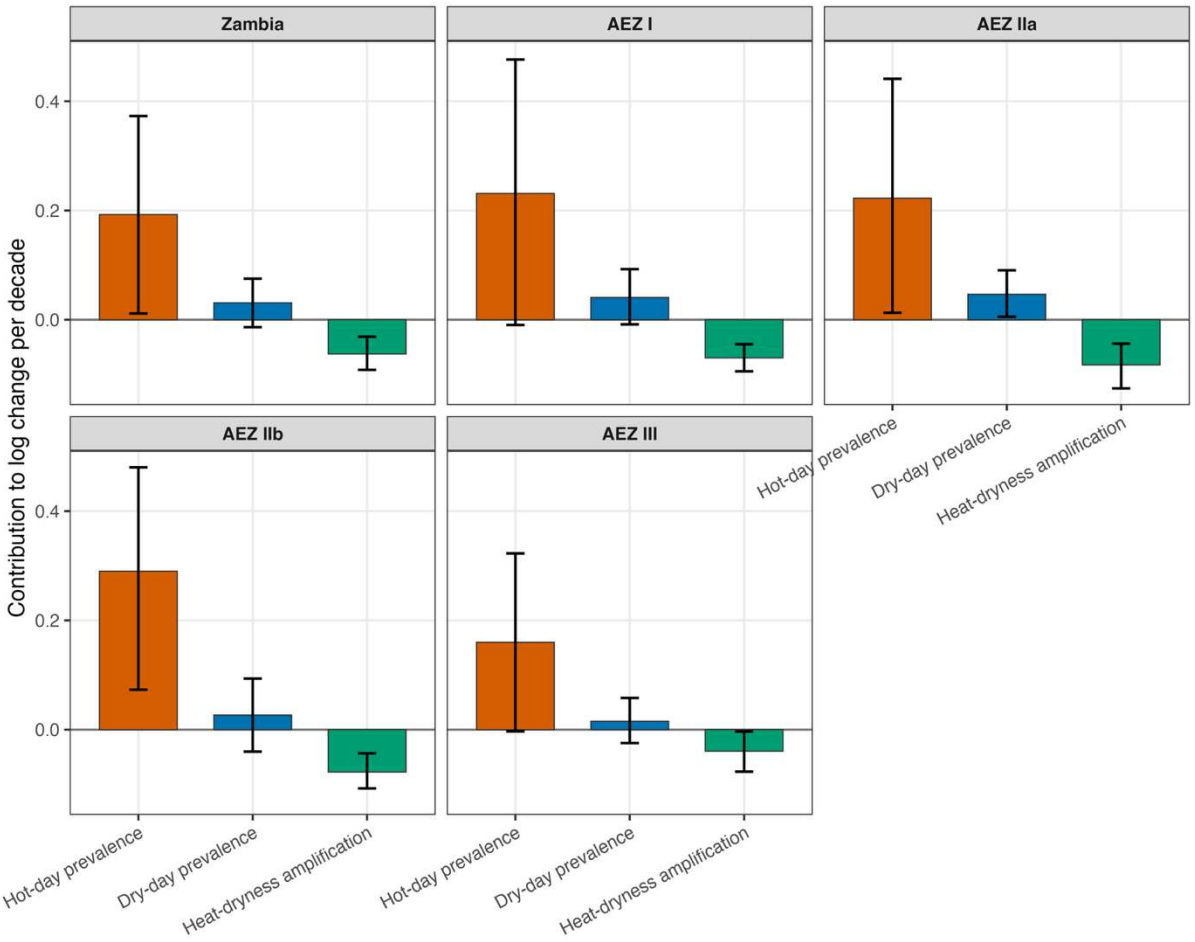


Figure 5: Decomposition of changes in joint hot-dry occurrence. Bars show contributions from hot-day prevalence, dry-day prevalence and regionally aggregated amplification. Error bars denote 95% joint moving-block bootstrap intervals.

3.4 High event burden did not require high amplification

Event burden and amplification occupied distinct seasonal states (Figure 6). Of the 30 seasons, eight combined high burden with low amplification, seven were high in both dimensions, eight had low burden and high amplification, and seven were low in both. The near-balanced distribution shows that burden and amplification describe different properties of compound hazards.

The 2023/24 season provided the clearest contrast. It contained 21.62 national hot-dry days, with hot-day, dry-day and joint probabilities of 0.281, 0.540 and 0.204, respectively. Its amplification ratio was 1.346, below the national median of approximately 1.79, placing the season in the high-burden, low-amplification state.

Major El Niño seasons did not occupy a common state. The 1997/98 season had low burden and high amplification, whereas 2015/16 and 2023/24 combined high burden with low amplification (Figure 6). Thus, seasons subject to similar large-scale climate forcing could differ substantially in the balance between marginal hazard prevalence and heat-dryness dependence. The four states are descriptive categories defined by sample medians and do not represent agronomic or impact thresholds.

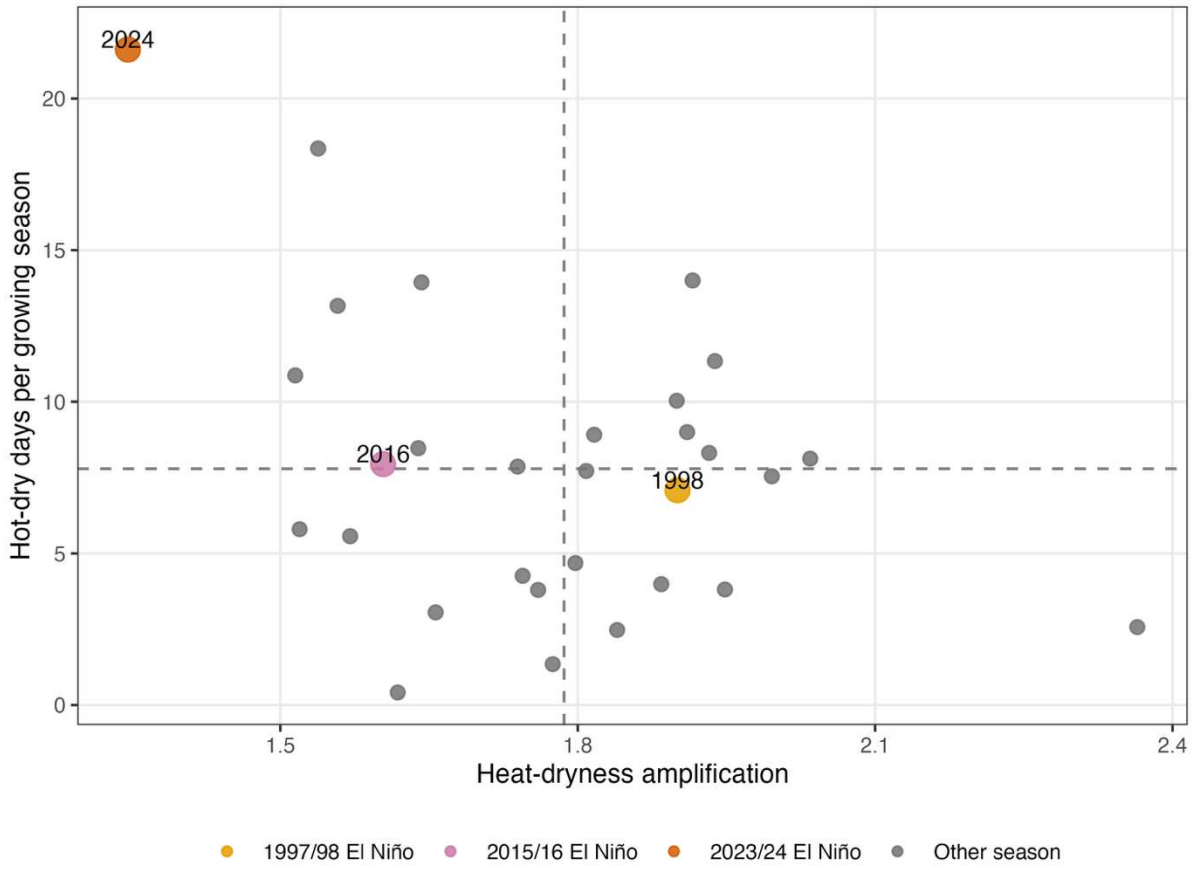


Figure 6: Burden and amplification across Zambia's growing seasons. Points represent seasons ending in 1996–2025. Dashed lines show sample medians defining four descriptive states. Major El Niño seasons are highlighted.

3.5 Major El Niño seasons influenced the observed trends

The 2023/24 season was the most prominent high-burden season in the record. After adjustment for the underlying time trend and the post-2015 period, it was associated with 1.91 additional events (95% CI, 0.92-2.91), 13.29 additional hot-dry days (95% CI, 5.03-21.56), 6.27 additional days of maximum duration (95% CI, 0.97-11.57) and 24.59 additional severity units (95% CI, 2.18-47.01). It also increased the probability of a season containing both a hot-dry event and a dry-to-wet transition by 0.194 ($p = 0.013$).

Despite this high burden, amplification in 2023/24 was lower by 0.460 (95% CI, −0.759 to −0.161; $p = 0.004$). Amplification was also lower in 2015/16 (−0.379; 95% CI, −0.680 to −0.079), although its estimated associations with event frequency, affected days, duration and severity were uncertain. These seasons reinforce the distinction between an increase in absolute burden and a strengthening of dependence.

The national amplification trend remained negative after excluding 1997/98, 2015/16 or 2023/24 individually, with slopes of −0.080, −0.081 and −0.061 per decade, respectively (Figure 7). Statistical support remained after excluding 1997/98 ($p = 0.022$) or 2015/16 ($p = 0.014$), but was borderline after excluding 2023/24 ($p = 0.051$). When all three seasons were excluded, the national slope weakened to −0.045 per decade and was no longer statistically supported ($p = 0.149$). AEZ I retained a supported decline after the joint exclusion (−0.104 per decade; $p = 0.010$). The national trend was therefore not attributable to a single El Niño season, but its magnitude and statistical strength were partly shaped by their combined influence.

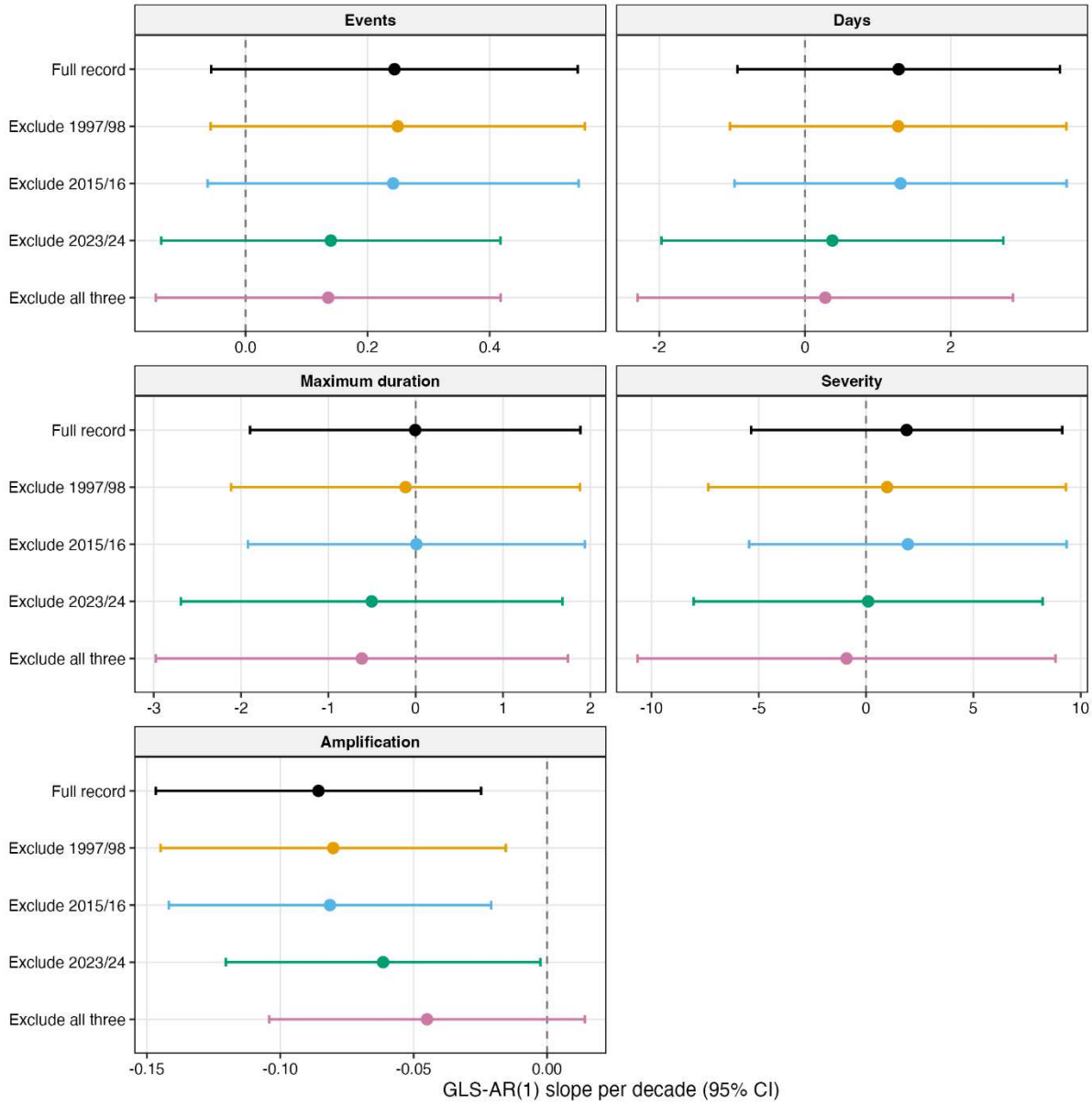


Figure 7:Sensitivity of GLS-AR(1) trends to exclusion of the 1997/98, 2015/16 and 2023/24 major El Niño seasons. Points show slopes per decade and intervals show uncertainty.

3.6 Sensitivity analyses

Restricting the analysis to a fixed geographical domain produced estimates that were nearly identical to those of the primary analysis. The common domain retained 98.06% of Zambia and at least 97.34% of each agro-ecological zone. All 35 national and regional trends retained their direction, and every common-domain confidence interval overlapped the corresponding primary interval.

National amplification declined by -0.0929 per decade on the common domain, compared with -0.0923 in the primary analysis. Corresponding estimates were −0.1063 versus −0.1065 in AEZ I and −0.1417 versus −0.1410 in AEZ IIa. An independent CDO analysis estimated a national decline of −0.0875 per decade, consistent with the Sen (−0.0923) and GLS (−0.0857) estimates. No discontinuity around 2015 was detected in mean temperature, unusually high temperature or CHIRPS rainfall.

Alternative event definitions produced trends of 0.130-0.347 events per decade and 0.450-1.705 hot-dry days per decade. All confidence intervals crossed zero. Duration trends remained close to zero, while severity trends were positive but uncertain.

The amplification decline persisted under alternative heat thresholds. Estimated declines were −0.080 per decade under P85 (95% CI, −0.131 to −0.029), −0.086 under P90 (95% CI, −0.149 to −0.022) and −0.101 under P95 (95% CI, −0.186 to −0.016). The P95 analysis had reduced effective coverage in some seasons and was therefore not fully comparable with the primary national estimate.

Excluding 2023/24 weakened evidence for nonlinear change in event frequency from $p = 0.007$ to $p = 0.056$ and reduced the fitted 1996-2025 difference from 0.801 to 0.405 events. The fitted difference in hot-dry days changed from +2.54 to −0.68 days, while the amplification decline weakened from −0.253 ($p = 0.020$) to −0.188 ($p = 0.115$). The principal directional findings were therefore robust to data coverage and event definition, but the fitted nonlinear trajectories remained sensitive to the exceptional 2023/24 season.

4 Discussion

4.1 Hazard burden and dependence represent distinct dimensions

Hot-dry event burden and heat-dryness amplification followed different trajectories across Zambia. Event frequency, affected days, duration and severity varied markedly among seasons but showed no consistent linear increase between 1996 and 2025. By contrast, amplification declined nationally, with the clearest evidence in AEZ I and AEZ IIa. High-burden seasons could therefore occur even as the excess co-occurrence of heat and dryness weakened.

Compound-event probability reflects both the prevalence of the contributing hazards and the dependence between them (Leonard et al. 2014; Zscheischler et al. 2018; Zscheischler et al. 2020). Previous studies have separated marginal and dependence contributions to changes in compound flooding and other multivariate extremes (Bevacqua et al. 2019; François and Vrac 2023). This study extends that reasoning from joint probability to realized seasonal burden by considering event frequency, affected days, duration, severity and temporal clustering. The distinction matters because equal joint probabilities can produce different burdens when hazardous days occur as isolated episodes or as persistent spells.

The decomposition indicates that the observed evolution of Zambia's hot-dry hazard was primarily associated with increasing hot-day prevalence. Dry-day prevalence made a smaller and less certain contribution, while declining amplification partly offset the heat-related increase. The resulting change in joint occurrence remained statistically unresolved. The evidence therefore points to a reorganization of the hazard components rather than a uniform rise in the probability of joint hot-dry conditions.

This interpretation also clarifies the meaning of amplification. Amplification is not a measure of event severity or damage. It measures how often heat and dryness coincide relative to the frequency expected from their separate occurrence. Event burden instead describes how much hazard was experienced through the number, persistence and intensity of qualifying events. A declining amplification ratio can therefore coexist with substantial or increasing exposure when hot conditions become more common.

The burden-amplification framework consequently adds information that is lost when compound hazards are represented by a single index. A high-burden season may arise

because one or both component hazards have become widespread, because their dependence has strengthened, or because hazardous days have clustered into persistent events. Distinguishing these pathways improves interpretation without assigning physical causation prematurely.

The decomposition remains statistical rather than causal. Increasing hot-day prevalence may reflect regional warming, circulation variability, land-surface processes and soil-moisture feedbacks, while changes in amplification may arise from shifts in the timing or spatial overlap of heat and rainfall deficits. Establishing these mechanisms will require soil-moisture observations, circulation diagnostics and counterfactual climate-model experiments. The contribution here is to identify the structure of observed compound-hazard change before attributing it to particular physical drivers.

4.2 Spatial structure and climate variability

National estimates concealed substantial geographical variation. Zambia spans strong gradients in rainfall, temperature, elevation and growing-season water availability, making a spatially uniform hot-dry response unlikely. The clearest regional declines in amplification occurred in the drier AEZ I and the agriculturally important AEZ IIa, whereas evidence was less consistent in AEZ IIb and weak in the wetter AEZ III. The national signal was therefore not produced equally across the four agro-ecological zones.

The spatial results further show that burden and dependence had different geographical expressions (Figure 4). Increases in event frequency were concentrated mainly in southern and southeastern Zambia. Hot-dry days and severity showed a broader contrast, with positive slopes across much of southern and south-central Zambia and negative slopes across parts of the north and northeast. Amplification exhibited a more coherent negative tendency across western, central and southern Zambia, together with localized positive slopes in parts of the north and northeast.

The geographical extent of a directional trend must nevertheless be distinguished from the area over which that trend was statistically resolved. Field-significant amplification declines covered 10.57% of Zambia, while significant increases covered only 0.23%. Significant declines were therefore concentrated in localized clusters within a much larger region characterized by negative slopes. For event frequency, hot-dry days and severity, very few cells passed the field-wide significance criterion. These results do not imply stability across the remaining area. Rather, they show that only a limited proportion of local trends could be separated confidently from strong interannual variability using 30 seasonal observations and spatially corrected inference.

Regional aggregation and grid-cell analysis consequently provide complementary evidence. National and AEZ estimates improve statistical precision by averaging across space but can obscure local contrasts. Grid-cell estimates preserve geographical heterogeneity but have lower power after adjustment for multiple testing. The regional results should therefore be interpreted as broad climatic tendencies, while the maps identify where local signals were sufficiently coherent to withstand field-wide correction.

ENSO added a further source of temporal and spatial structure. The major El Niño seasons ending in 1998, 2016 and 2024 occupied different positions in the burden-amplification plane. The 1997/98 season exhibited comparatively low burden and high amplification, whereas 2015/16 and 2023/24 combined high burden with relatively low amplification. A shared El Niño classification therefore did not produce a uniform compound-hazard response across Zambia.

This diversity is consistent with the variable expression of southern African ENSO teleconnections. Regional outcomes depend not only on the presence of El Niño but also on the magnitude, location and seasonal evolution of Pacific warming and its interaction with Indian Ocean conditions and regional atmospheric circulation (Hoell et al. 2015). Compound extremes can further emerge through interactions among large-scale climate modes, antecedent land conditions and regional processes (Raymond et al. 2020). ENSO provides an important source of seasonal predictability, but it is not a deterministic indicator of either hot-dry burden or heat-dryness amplification.

The leave-out analysis strengthens this interpretation. Removing any one of the three major El Niño seasons preserved the negative direction of the national amplification trend, although its precision varied. Removing all three together substantially weakened the trend. No single event generated the decline, but the major El Niño seasons collectively contributed to its magnitude. Its attenuation after their joint exclusion limits interpretation as a secular change independent of ENSO variability.

The observed amplification trend should therefore be understood as a property of the complete climate record, in which interannual variability and longer-term change remain difficult to separate over three decades. Climate-model evidence suggests that ENSO teleconnections to southern Africa may persist under continued warming, although their future strength and geographical expression remain uncertain (Steinkopf and Engelbrecht 2025). Extrapolating the observed decline in amplification beyond the study period would consequently be premature.

4.3 Implications for compound-hazard monitoring

Compound-hazard monitoring should distinguish three questions. How common were the individual hazards? How much event burden occurred? Did the hazards coincide more frequently than expected from their separate prevalence? These questions correspond to marginal prevalence, realized event burden and amplification. Reporting them separately would reveal whether a changing hazard is driven by more frequent heat, more frequent dryness, stronger dependence or greater temporal clustering.

An operational monitoring product could first report the prevalence of hot and dry days, followed by event frequency, affected days, duration and severity. Amplification could then indicate whether heat and dryness coincided disproportionately, while decomposition would identify which component contributed most strongly to observed change. This structure retains indicators that users can interpret directly while preserving information about the statistical organization of the compound hazard.

Such an approach addresses growing concern that warning systems organized around individual hazards may fail to represent interactions, sequences and shared drivers of compound disasters (Alcântara and Mantovani 2026). A burden-amplification framework would distinguish seasons dominated by widespread component hazards from those characterized by unusually strong dependence. It would also prevent a declining association measure from being misinterpreted as declining exposure.

The distinction has particular relevance for agriculture. Event duration and affected days can be aligned with crop establishment, flowering and grain filling, while amplification describes the dependence structure underlying those conditions. Climate-model analyses indicate that interacting heat and water limitations threaten rainfed maize production in Zambia (Siatwiinda et al. 2021), and participatory research identifies heat stress as an under-addressed constraint on smallholder adaptation (Nyambe 2024; Siatwiinda et al. 2026). Separating burden from dependence offers a

clearer basis for investigating how these climatic pressures translate into crop and livelihood outcomes.

Meteorological hazard is not equivalent to impact. Across Africa, the consequences of heat, drought and rainfall extremes depend on exposure, livelihood sensitivity, infrastructure and adaptive capacity (Trisos 2022). Similar hot-dry conditions may therefore produce different outcomes among crops, farming systems and agro-ecological zones. Operational thresholds should be calibrated against crop phenology, yields, streamflow and livelihood outcomes rather than derived from the sample medians used here. The four burden-amplification states are descriptive tools for comparing seasons, not validated thresholds of agricultural or societal risk.

Spatial scale also requires careful consideration. National averages may conceal opposing regional changes, whereas individual grid-cell estimates may be too uncertain for routine decisions. Agro-ecological summaries provide an intermediate scale that is statistically more stable and relevant to agricultural planning. Future monitoring systems could combine these regional summaries with spatial maps and explicit uncertainty estimates.

The framework is transferable beyond hot-dry hazards. Where joint occurrence can be represented through marginal probabilities and an association term, the same logic could be applied to hot-humid conditions, drought and fire weather, or extreme rainfall and storm surge. Transferability does not imply universal indicators or thresholds. Variables, temporal windows and event structures must be selected according to the physical interaction and impact process under investigation (Zscheischler et al. 2020; Leonard et al. 2014; Bevacqua et al. 2021).

4.4 Robustness, interpretation and limitations

Confidence in the central interpretation arises from agreement across complementary methods rather than from any single significance test. Sen slopes, modified Mann-Kendall tests, autocorrelation-adjusted regression and block-bootstrap intervals addressed different properties of a short and variable climatic record. Alternative event definitions, a fixed common spatial domain and an independent Climate Data Operators calculation produced consistent directional evidence for declining amplification. The principal result was therefore unlikely to have arisen solely from one estimator, one event definition or the post-2015 change in ERA5-Land coverage.

The strength of evidence was nevertheless asymmetric. Increasing hot-day prevalence and declining amplification were more consistently supported than the net change in joint occurrence. The positive estimate for joint occurrence should therefore not be presented as evidence of a uniform national increase. Equally, an interval spanning zero does not demonstrate an absence of change; it indicates that the direction and magnitude could not be resolved confidently from the available record.

Nonlinear burden trajectories require similar restraint. Smooth curves fitted to 30 seasons describe variation within the observed record rather than a stable physical process. Their sensitivity to the exceptional 2023/24 season shows that inferred trajectory shapes can be strongly influenced by individual events. The models demonstrate that a straight line provides an incomplete summary of the record, but they do not establish a persistent pathway or support extrapolation beyond 2025.

The findings also depend on the selected event definition and aggregation scale. Alternative temperature percentiles and spell requirements preserved the main interpretation, but no finite sensitivity analysis can represent every impact-relevant definition. The strictest heat threshold reduced effective spatial coverage during seasons with few extreme hot days. Regional amplification calculated from aggregated

probabilities also differs conceptually from an area-weighted mean of cell-level ratios. The former preserves the exact decomposition identity, whereas the latter represents average local dependence. These measures answer related but different questions.

Uncertainty in the underlying climate products remains an additional limitation. CHIRPS combines satellite rainfall estimates with gauge observations, while ERA5-Land is a model-based reanalysis (Funk et al. 2015; Muñoz-Sabater et al. 2021). Common-grid processing and fixed-domain analysis improved comparability but cannot eliminate biases in rainfall detection, near-surface temperature or topographic representation. Evaluation against station observations and additional gridded products would provide a valuable independent test where sufficiently complete records are available.

Finally, the analysis diagnoses climatic hazard rather than its consequences. It does not establish effects on crop yields, livestock, hydropower production or household welfare. Linking burden and amplification to observed impacts is necessary before the framework can support operational warning thresholds. Future work should also test whether the observed divergence between burden and amplification persists under warming using bias-aware daily climate simulations that preserve marginal distributions, dependence and temporal event structure.

5 Conclusion

Compound hot-dry hazards changed through distinct and partly opposing pathways across Zambia between 1996 and 2025. Event frequency, affected days, duration and severity varied strongly among seasons but did not show a uniform long-term increase. Heat-dryness amplification declined nationally, most clearly in AEZ I and AEZ IIa, although the signal was spatially concentrated and partly shaped by major El Niño seasons.

Decomposition showed that increasing hot-day prevalence was the dominant positive component of change in joint hot-dry occurrence. Dry-day prevalence changed comparatively little, while declining amplification offset part of the increase associated with more frequent hot conditions. The resulting trend in joint occurrence remained uncertain. High-burden seasons therefore did not necessarily reflect stronger heat-dryness dependence, as demonstrated most clearly by the 2023/24 season.

These findings support a broader analytical principle. Changes in compound-hazard burden should be separated from changes in dependence. Event counts and affected days describe how much hazard occurred, whereas amplification identifies whether the component hazards coincided more often than expected from their separate frequencies. Monitoring either dimension alone can obscure the structure of change.

Compound-hazard assessments should therefore report marginal hazard prevalence, event burden and amplification together. This framework is transferable to other multivariate hazards, but its operational use requires calibration against observed impacts. For Zambia, linking these metrics with crop phenology, production losses, streamflow and livelihood outcomes is the next step towards impact-based early warning. Whether the observed weakening of heat-dryness amplification persists under future warming remains unresolved and should be tested using bias-aware daily climate-model simulations.

Declarations

Acknowledgements: The author thanks Dr. Chesu Chisala for reviewing an earlier version of the manuscript and providing constructive comments.

Funding: This research received no external funding.

Conflicts of interest/Competing interests: The author declares no competing financial or non-financial interests.

Ethical Approval: This study used publicly available gridded climate data and did not involve human participants, personal data, animals or biological materials. Ethical approval and informed consent were therefore not required.

Author Contributions: SMS- Conceptualization, data analysis, and manuscript drafting.

Consent to publish: Not applicable**.**

Data Availability Statement: CHIRPS v2 daily rainfall data are publicly available from the Climate Hazards Center at https://data.chc.ucsb.edu/products/CHIRPS-2.0/africa_daily/ , and ERA5-Land hourly data are available through the Copernicus Climate Data Store at https://cds.climate.copernicus.eu/datasets/reanalysis-era5-land?tab=download.

Code availability: The scripts used in data analysis are readily available on request.

6 References

AghaKouchak A, Chiang F, Huning LS, Love CA, Mallakpour I, Mazdiyasni O, Moftakhari H, Papalexiou SM, Ragno E, Sadegh M (2020) Climate extremes and compound hazards in a warming world. Annual review of earth and planetary sciences 48 (1):519-548. doi:https://doi.org/10.1146/annurev-earth-071719-055228

Akaike H (1974) A new look at the statistical model identification. IEEE Transactions on Automatic Control 19 (6):716-723. doi:https://doi.org/10.1109/TAC.1974.1100705

Al-Wardy M, Zarei E, Nikoo MR, Al-Balushi M (2026) Assessing compound drought-heatwave events in Oman using non-stationary copula models. Journal of Hydrology 679:136149. doi:https://doi.org/10.1016/j.jhydrol.2026.136149

Alcântara E, Mantovani JR (2026) Early-warning systems unfit for compound disasters. Discover Hazards 2 (1):43. doi:https://doi.org/10.1007/s44475-026-00052-1

Benjamini Y, Hochberg Y (1995) Controlling the False Discovery Rate: A Practical and Powerful Approach to Multiple Testing. Journal of the Royal Statistical Society: Series B (Methodological) 57 (1):289-300. doi:https://doi.org/10.1111/j.2517-6161.1995.tb02031.x

Bevacqua E, De Michele C, Manning C, Couasnon A, Ribeiro AFS, Ramos AM, Vignotto E, Bastos A, Blesić S, Durante F, Hillier J, Oliveira SC, Pinto JG, Ragno E, Rivoire P, Saunders K, van der Wiel K, Wu W, Zhang T, Zscheischler J (2021) Guidelines for Studying Diverse Types of Compound Weather and Climate Events. Earth's Future 9 (11):e2021EF002340. doi:https://doi.org/10.1029/2021EF002340

Bevacqua E, Maraun D, Vousdoukas MI, Voukouvalas E, Vrac M, Mentaschi L, Widmann M (2019) Higher probability of compound flooding from precipitation and storm surge in Europe under anthropogenic climate change. Science Advances 5 (9):eaaw5531. doi:https://doi.org/10.1126/sciadv.aaw5531

Cao H, Yang Q, Yang W, Zhao L (2025) China's three major cereal crops exposed to compound drought and extreme rainfall events. Natural Hazards and Earth System Sciences 25 (12):5017-5031. doi:https://doi.org/10.5194/nhess-25-5017-2025

Chisanga CB, Nkonde E, Mubanga KH, Phiri D, Chemura A, Kipkulei HK (2025) SPI-based drought characteristics using CHIRPS over Zambia: 1981–2024. All Earth 37 (1):1-19. doi:https://doi.org/10.1080/27669645.2025.2472574

Chisanga CB, Nkonde E, Phiri E, Mubanga KH, Lwando C (2023) Trend analysis of rainfall from 1981-2022 over Zambia. Heliyon 9 (11). doi:https://doi.org/10.1016/j.heliyon.2023.e22345

Ebi KL (2025) Understanding the risks of compound climate events and cascading risks. Dialogues on Climate Change 2 (1):33-37. doi:https://doi.org/10.1177/29768659241304857

François B, Vrac M (2023) Time of emergence of compound events: contribution of univariate and dependence properties. Natural Hazards and Earth System Sciences 23 (1):21-44. doi:https://doi.org/10.5194/nhess-23-21-2023

Funk C, Peterson P, Landsfeld M, Pedreros D, Verdin J, Shukla S, Husak G, Rowland J, Harrison L, Hoell A (2015) The climate hazards infrared precipitation with stations—a new environmental record for monitoring extremes. Scientific data 2 (1):150066. doi:https://doi.org/10.1038/sdata.2015.66

Hachigonta S, Reason C, Tadross M (2008) An analysis of onset date and rainy season duration over Zambia. Theoretical and Applied Climatology 91 (1):229-243. doi:https://doi.org/10.1007/s00704-007-0306-4

Hamed KH, Ramachandra Rao A (1998) A modified Mann-Kendall trend test for autocorrelated data. Journal of Hydrology 204 (1):182-196. doi:https://doi.org/10.1016/S0022-1694(97)00125-X

Hamududu BH, Ngoma H (2019) Impacts of climate change on water availability in Zambia: Implications for irrigation development. doi:https://doi.org/10.13140/RG.2.2.10265.72805

Hao Z, Hao F, Singh VP, Zhang X (2018a) Quantifying the relationship between compound dry and hot events and El Niño–southern Oscillation (ENSO) at the global scale. Journal of Hydrology 567:332-338. doi:https://doi.org/10.1016/j.jhydrol.2018.10.022

Hao Z, Singh VP, Hao F (2018b) Compound extremes in hydroclimatology: a review. Water 10 (6):718. doi:https://doi.org/10.3390/w10060718

He B, Zhong Z, Chen D, Liu J, Chen Y, Miao C, Ding R, Yuan W, Guo L, Huang L, Hao X, Chen A (2022) Lengthening Dry Spells Intensify Summer Heatwaves. Geophysical Research Letters 49 (19):e2022GL099647. doi:https://doi.org/10.1029/2022GL099647

Hoell A, Funk C, Magadzire T, Zinke J, Husak G (2015) El Niño–Southern Oscillation diversity and Southern Africa teleconnections during Austral Summer. Climate Dynamics 45 (5):1583-1599. doi:https://doi.org/10.1007/s00382-014-2414-z

Leonard M, Westra S, Phatak A, Lambert M, van den Hurk B, McInnes K, Risbey J, Schuster S, Jakob D, Stafford-Smith M (2014) A compound event framework for understanding extreme impacts. Wiley Interdisciplinary Reviews: Climate Change 5 (1):113-128. doi:https://doi.org/10.1002/wcc.252

Lesk C, Anderson W, Rigden A, Coast O, Jägermeyr J, McDermid S, Davis KF, Konar M (2022) Compound heat and moisture extreme impacts on global crop yields under climate change. Nature Reviews Earth & Environment 3 (12):872-889. doi:https://doi.org/10.1038/s43017-022-00368-8

Libanda B, Bwalya K, Nkolola NB, Chilekana N (2020) Quantifying long-term variability of precipitation and temperature over Zambia. Journal of Atmospheric and Solar-Terrestrial Physics 198:105201. doi:https://doi.org/10.1016/j.jastp.2020.105201

Lyon B (2009) Southern Africa Summer Drought and Heat Waves: Observations and Coupled Model Behavior. Journal of Climate 22 (22):6033-6046. doi:https://doi.org/10.1175/2009JCLI3101.1

Majid M, Fethi L (2024) The characterization of droughts and dry spells in Northern Tunisia based on the analysis of daily rainfall series. Journal of Hydrology: Regional Studies 56:102047. doi:https://doi.org/10.1016/j.ejrh.2024.102047

Moses O, Kupika OL, Hambira WL, Gondwe M (2025) A comparison of the 2023/24 El Niño with other El Niño events during 1981—2024 over the Okavango River Basin, southern Africa. Theoretical and Applied Climatology 156 (7):373. doi:https://doi.org/10.1007/s00704-025-05593-x

Mulungu K, Nyirenda Z, Nakamba B, Ngoma H (2026) Crop-specific impacts of the 2023/2024 drought on Zambia's agricultural production. Climate Services 44:100710. doi:https://doi.org/10.1016/j.cliser.2026.100710

Muñoz-Sabater J, Dutra E, Agustí-Panareda A, Albergel C, Arduini G, Balsamo G, Boussetta S, Choulga M, Harrigan S, Hersbach H, Martens B, Miralles DG, Piles M, Rodríguez-Fernández NJ, Zsoter E, Buontempo C, Thépaut JN (2021) ERA5-Land: a state-of-the-art global reanalysis dataset for land applications. Earth Syst Sci Data 13 (9):4349-4383. doi:https://doi.org/10.5194/essd-13-4349-2021

Nyambe A (2024) Exploring climate change perception and heat stress adaptation among Zambian farmers using participatory tools. Regional Environmental Change 24 (2):46. doi:https://doi.org/10.1007/s10113-024-02206-7

Pinheiro JC, Bates DM (2000) Mixed-effects models in S and S-PLUS. Springer. doi:https://doi.org/10.1007/b98882

Raymond C, Horton RM, Zscheischler J, Martius O, AghaKouchak A, Balch J, Bowen SG, Camargo SJ, Hess J, Kornhuber K, Oppenheimer M, Ruane AC, Wahl T, White K (2020) Understanding and managing connected extreme events. Nature Climate Change 10 (7):611-621. doi:https://doi.org/10.1038/s41558-020-0790-4

Schulzweida U, Kornblueh L, Quast R (2019) CDO user guide. Zenodo,

Siatwiinda SM, Kunda C, Scott S, Muchochoma D, Mwondela MgD, Nkhoma CJ, Chisala C, Mwalishinka O, Chooma B, Msukwa C (2026) Balancing biological performance, profitability and external feed dependency in farmer managed broiler systems in Zambia. Discover Agriculture 4 (1):261. doi:https://doi.org/10.1007/s44279-026-00739-5

Siatwiinda SM, Supit I, van Hove B, Yerokun O, Ros GH, de Vries W (2021) Climate change impacts on rainfed maize yields in Zambia under conventional and optimized crop management. Climatic Change 167 (3):39. doi:https://doi.org/10.1007/s10584-021-03191-0

Sparrow S, Perez-Fernandez I, Tett S (2026) Attribution study of the 2023-2024 Drought on the South of Africa. Copernicus Meetings. doi:https://doi.org/10.5194/egusphere-egu26-23150

Steinkopf J, Engelbrecht F (2025) The El Niño–Southern Oscillation teleconnection to southern Africa in a changing climate. Environmental Research Letters 20 (8):084001. doi:https://doi.org/10.1088/1748-9326/ade60e

Szalińska W, Otop I, Tokarczyk T (2021) Local urban risk assessment of dry and hot hazards for planning mitigation measures. Climate Risk Management 34:100371. doi:https://doi.org/10.1016/j.crm.2021.100371

Tirivarombo S, Osupile D, Eliasson P (2018) Drought monitoring and analysis: standardised precipitation evapotranspiration index (SPEI) and standardised precipitation index (SPI). Physics and Chemistry of the Earth, Parts a/b/c 106:1-10. doi:https://doi.org/10.1016/j.pce.2018.07.001

Trisos CHA, I. O.; Totin, E.; Ayanlade, A.; Efitre, J.; Gemeda, A.; Kalaba, K.; Lennard, C.; Masao, C.; Mgaya, Y.; Ngaruiya, G.; Olago, D.; Simpson, N. P.; Zakieldeen, S. (2022) Africa. In: Pörtner H-OR, D. C.; Tignor, M.; Poloczanska, E. S.; Mintenbeck, K.; Alegría, A.; Craig, M.; Langsdorf, S.; Löschke, S.; Möller, V.; Okem, A.; Rama, B. (ed) Climate Change 2022: Impacts, Adaptation and Vulnerability. . Contribution of Working Group II to the Sixth Assessment Report of the Intergovernmental Panel on Climate Change Cambridge, pp 1285–1455. doi:https://doi.org/10.1017/9781009325844.011

Trnka M, Semerádová D, Novotný I, Dumbrovský M, Drbal K, Pavlík F, Vopravil J, Štěpánková P, Vizina A, Balek J (2016) Assessing the combined hazards of drought, soil erosion and local flooding on agricultural land: a Czech case study. Climate Research 70:231-249. doi:https://doi.org/10.3354/cr01421

Vogel K, Sieg T, Veh G, Fiedler B, Moran T, Peter M, Rottler E, Bronstert A (2024) Natural Hazards in a Changing World: Methods for Analyzing Trends and Non-Linear Changes. Earth's Future 12 (5):e2023EF003553. doi:https://doi.org/10.1029/2023EF003553

White CJ, Adnan MSG, Arosio M, Buller S, Cha Y, Ciurean R, Crummy JM, Duncan M, Gill J, Kennedy C, Nobile E, Smale L, Ward PJ (2025) Review article: Towards multi-hazard and multi-risk indicators – a review and recommendations for development and implementation. Nat Hazards Earth Syst Sci 25 (11):4263-4281. doi:https://doi.org/10.5194/nhess-25-4263-2025

Wilks DS (1997) Resampling Hypothesis Tests for Autocorrelated Fields. Journal of Climate 10 (1):65-82. doi:https://doi.org/10.1175/1520-0442(1997)010<0065:RHTFAF>2.0.CO;2

Wood SN (2025) Generalized additive models. Annual Review of Statistics and Its Application 12 (1):497-526. doi:https://doi.org/10.1146/annurev-statistics-112723-034249

Zhang Y, Hao Z, Jiang Y, Singh VP (2023) Global warming increases risk from compound dry-hot events to human and agricultural systems. International Journal of Climatology 43 (14):6706-6719. doi:https://doi.org/10.1002/joc.8229

Zscheischler J, Martius O, Westra S, Bevacqua E, Raymond C, Horton R, Hurk B, AghaKouchak A, Jézéquel A, Mahecha M, Maraun D, Ramos A, Ridder N, Thiery W, Vignotto E (2020) A typology of compound weather and climate events. Nature Reviews Earth & Environment 1:333-347. doi:https://doi.org/10.1038/s43017-020-0060-z

Zscheischler J, Westra S, Van Den Hurk BJ, Seneviratne SI, Ward PJ, Pitman A, AghaKouchak A, Bresch DN, Leonard M, Wahl T (2018) Future climate risk from compound events. Nature Climate Change 8 (6):469-477. doi:https://doi.org/10.1038/s41558-018-0156-3